

Received August 16, 2020; reviewed; accepted October 29, 2020

Comparison study of crystal and electronic structures for chalcopyrite (CuFeS₂) and pyrite (FeS₂)

Yuqiong Li ^{1,2}, Yingchao Liu ³, Jianhua Chen ^{1,2}, Cuihua Zhao ², Weiyong Cui ³

¹ Guangxi Key Laboratory of Processing for Non-ferrous Metal and Featured Materials, Guangxi University, Nanning, China

² School of Resources, Environment and Materials, Guangxi University, Nanning, China

³ School of Chemistry and Chemical Engineering, Guangxi University, Nanning, China

Corresponding author: jhchen@gxu.edu.cn (J. Chen)

Abstract: Chalcopyrite (CuFeS₂) and pyrite (FeS₂) are commonly associated with each other, and they both belong to semiconductor minerals. The difference in crystal and electronic structures is an important factor for their flotation separation. Using the density functional method (DFT) combined with Hubbard U correction, their crystal and electronic properties are comparatively studied. The calculated results suggest that the use of antiferromagnetic calculations and Hubbard U correction are very important to the accuracy of the chalcopyrite results. Antiferromagnetic calculations combined with a U value of 2.0 eV on chalcopyrite show a band gap of 0.53 eV, which is very consistent with the experimental results of ~0.5 eV. The density of states (DOS) and Mulliken bond population results indicate that stronger hybridization between Fe 3d and S 3p states in chalcopyrite than in pyrite leads to a stronger covalency of Fe-S bonds in chalcopyrite, causing a reduction in the spin magnetic moment (3.5 μB) from the ideal value. In addition, the greater covalency of bonds in chalcopyrite results in greater hydrophobicity of chalcopyrite than pyrite. The DOS results suggest that S has similar electronic properties in pyrite and chalcopyrite. The oxidation states of Fe and Cu ions in chalcopyrite are discussed based on the coordination field theory according to the calculation results, which confirms an oxidation state of Fe³⁺Cu¹⁺S₂.

Keywords: chalcopyrite, pyrite, crystal structures, electronic structures

1. Introduction

Pyrite (FeS₂) is the most common sulphide in nature and has received more attention due to its wide application, and it is commonly associated with chalcopyrite (CuFeS₂) (Mu et al., 2018). Pyrite has attracted the interest of scientists as a photovoltaic and photoelectric material due to its suitable band gap and strong light absorption coefficient (Yu et al., 2011; Nakamura et al., 2001). Chalcopyrite materials also have received considerable interest as solar cell materials (Park et al., 2014; Hiroi et al., 2015). Chalcopyrite and pyrite have similar properties, such as narrow gap semiconductor sulphide minerals. In addition, the resting potentials of pyrite and chalcopyrite in xanthate solution are measured to be very close (0.14 V for chalcopyrite and 0.22 V for pyrite). Moreover, after xanthate (X⁻) interacts with chalcopyrite and pyrite, dixanthate (X₂) is found on the surfaces of both chalcopyrite and pyrite (Allison et al., 1972). However, there are also some differences between them. Chalcopyrite crystals belong to tetragonal structures, while pyrite crystals belong to cubic structures. Some researchers have studied the crystal structures and electronic structures of pyrite and chalcopyrites (Li et al., 2015 and 2018; Siebentritt et al., 2010; Jaffe and Zunger, 1983). However, there is no in-depth study on the internal relations and differences between them. It is meaningful to study the differences between the two minerals' crystal properties, including crystal structure and electronic structure.

Cu and Fe are two of the first transition metal elements. The crystal structure of chalcopyrite is

relatively different from that of pyrite. Cu and Fe ions in chalcopyrite are four-coordinated by sulphur atoms, while Fe in pyrite is six-coordinated by sulphur atoms, forming tetrahedral fields and octahedral fields. Fe in a tetrahedral field and octahedral field will exhibit a large difference in bonding nature and electronic properties. Based on DFT simulations, Edelbro et al. (2003) studied the electronic structure of pyrite and chalcopyrite. They suggest that the bond covalence between transition metal elements (Cu and Fe atoms) and S atoms in chalcopyrite is stronger than that of Fe-S in pyrite. In addition, the Fe 3d state is metallic for pyrite, while chalcopyrite does not have this property.

Many experimental and theoretical studies have been reported on the magnetic and electronic properties of chalcopyrite and pyrite (Ennaoui et al., 1993; Conejeros et al., 2015; Teranishi, 1961; Lazewski et al., 2004; Zhou et al., 2015; Lyubutin et al., 2013; Klekovkina et al., 2014; Kradinova et al., 1999). Pyrite is suggested as a semiconductor with a narrow band gap, but chalcopyrite is suggested as a conductor or semiconductor. The experimentally determined band gap for chalcopyrite is very different from the DFT calculation results. Goodman and Douglas (1954) and Austin et al. (1956) suggested an ~0.5-eV band gap from experiments, whereas Kradinova et al. (1999) suggested CuFeS₂ as a zero-gap semiconductor. Density functional theory (DFT) calculations suggest a very wide range from 0 to 1.82 eV (Oliveira and Duarte, 2010; Martínez-Casado et al., 2016; Edelbro et al., 2003; Conejeros et al., 2015). Edelbro et al. (2003) proposed that the discrepancy between experimental and theoretical results is probably due to imperfect or modified materials, experimental conditions and the deficiency of theoretical calculations.

In addition, two ionic states for chalcopyrite, Cu⁺Fe³⁺S₂²⁻ and Cu²⁺Fe²⁺S₂²⁻, have been proposed based on X-ray spectroscopy (Ballal and Mande, 1978; Todd et al., 2003; Mikhlin et al., 2005) and the Mössbauer absorption spectrum (Aramu et al., 1967). Pauling and Brockway, based on X-ray experiments, established a mixture of the two extreme ionic states (Pauling and Brockway, 1932). Aramu et al. (1967) proposed that chalcopyrite may be represented by the resonant configuration Cu⁺Fe³⁺(S²⁻)-Cu³⁺Fe(S²⁻)₂. However, it is generally accepted that Cu ions belong to the monovalent copper class and that Fe ions belong to the trivalent class. The erroneous interpretation of Cu²⁺Fe²⁺S₂²⁻ may be ascribed to the simplistic measurement method (Pearce et al., 2006).

DFT-GGA calculations often underestimate the energy gap of materials. Hence, Hubbard U correction, as well as an antiferromagnetic property, were added to improve the DFT calculation as part of a thorough comparative study on the structural and electronic properties of pyrite and chalcopyrite, which has not previously been focused on. Additionally, the oxidation states of Cu and Fe are discussed and compared based on the coordination field theory according to the theoretical calculation results.

2. Computational models and methods

Chalcopyrite and pyrite mostly belong to tetragonal and cubic structures, and their symmetry groups are I4₂d and Pa3, respectively. Both Cu and Fe atoms in the chalcopyrite are coordinated by four S atoms, and S atoms are coordinated by two Fe atoms and two Cu atoms. These ions are formed in the tetragonal structure. In pyrite, each Fe atom is coordinated by six S atoms, forming an octahedral structure, and S atoms form a tetragonal structure with three Fe atoms and one S atom. The S₂²⁻ dimer (S1-S2), which has a dumbbell structure, is formed in pyrite. This is different from the situation in chalcopyrite. Fig. 1 shows the unit cells of these two crystals.

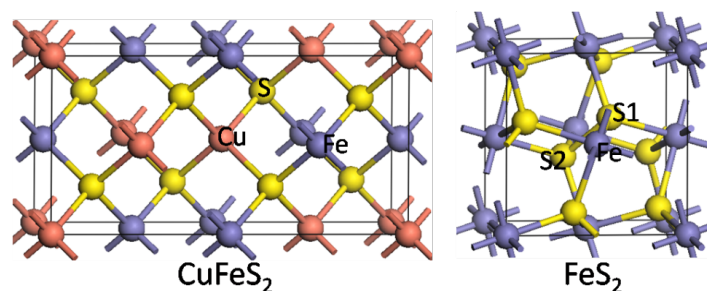


Fig. 1. Unit cells of chalcopyrite and pyrite

The calculations were performed by the CASTEP module (Clark et al., 2005), which is a first-principle method based on density-functional theory (DFT) (Xie and Lu, 1998; Marzari et al., 1997). Ultrasoft pseudopotentials were used to calculate the interaction between valence electrons and the ionic core. The self-consistent field convergence accuracy was set to 2.0×10^{-6} eV/atom. The displacement between two atoms was less than 2.0×10^{-3} Å. The convergence thresholds for the maximum energy change, force and stress during the geometry optimization were set to 2×10^{-5} eV/atom, 0.05 eV/Å and 0.1 GPa, respectively. The k-point was set to $4 \times 4 \times 4$ for pyrite and $4 \times 4 \times 2$ for chalcopyrite according to the Monkhorst-Pack method. Pseudo atomic calculations performed for Cu, Fe and S were $3d^{10}4s^1$, $3d^64s^2$ and $S 3s^2p^4$, respectively. The frontier orbital was calculated by using the DMol³ module. All electrons were included in the frontier orbital calculations, and the DNP atomic orbital basis set was used. GGA-PW91 was used for both CASTEP and DMol³ calculations as the exchange-correlation functional. Spin calculation was performed during the geometry optimization.

3. Results and discussion

3.1 Influence of Hubbard U correction on crystal structures

First, the energy cut-off used for the plane wave basis set was tested during geometry optimization. The tested results on pyrite are shown in Fig. 2. It is indicated that the total energy of pyrite decreases with increasing energy cut-off and changes gently when higher than 350 eV. Finally, an energy cut-off of 400 eV was determined.

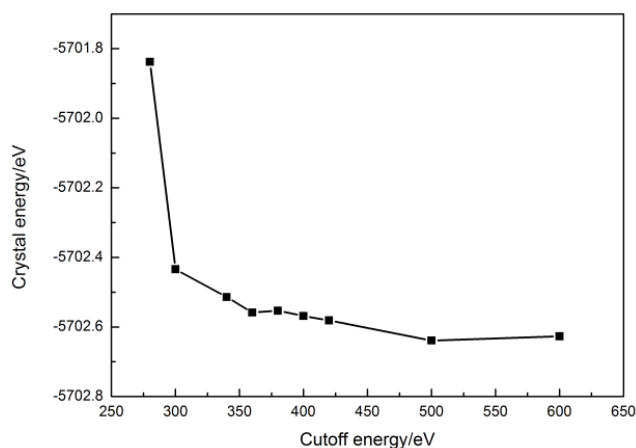


Fig. 2. Effect of cut-off energy on the total energy of pyrite

Pyrite crystals are paramagnetic in the low-spin configuration. Considering that the band gap given by GGA deviates too greatly from the experimental value, Hubbard U correction (Anisimov et al., 1991 and 1995) was adopted for the treatment of Fe 3d with strongly correlated electrons. The calculated band gap of pyrite can be improved from 0.55 eV at a U value of 0 eV to 1.01 eV at a U value of 1.5 eV. This result is very close to the experimental value of 0.95 eV (Schlegel and Wachter, 1976), suggesting that GGA+U can yield a better energy gap result than GGA. In addition, when a U value of 1.5 eV is adopted, the cell parameter of pyrite is 5.3778 Å, which is very close to the experimental value of 5.4160 Å (Prince et al., 2005).

However, the band gap of chalcopyrite is zero at any of the tested U values when chalcopyrite is in a ferromagnetic state. Hence, we performed an antiferromagnetic calculation for chalcopyrite at different U values. The direction of the spins of the iron ions is along the c axis (Conejeros et al., 2015; Donnay et al., 1958; Woolley et al., 1996; Rais et al., 2000). Table 1 shows the total energies of chalcopyrite in ferromagnetic and antiferromagnetic states. It is suggested that antiferromagnetic chalcopyrite is more stable than ferromagnetic chalcopyrite. Hence, chalcopyrite should be antiferromagnetic. This is consistent with the antiferromagnetic property of chalcopyrite (Conejeros et al., 2015; Donnay et al., 1958; Woolley et al., 1996; Rais et al., 2000; Engin et al., 2011; Knight et al., 2011; Pearce et al., 2006).

Table 2 shows the influences of U values on the cell parameters of antiferromagnetic chalcopyrite.

The cell parameters of chalcopyrite increase slightly when the Hubbard U correction increases. When the U value is 2.0 eV, $a=b=5.2927 \text{ \AA}$ and $c=10.3875 \text{ \AA}$ are the closest to the experimental results of $a=b=5.290 \text{ \AA}$ and $c=10.4217 \text{ \AA}$.

Table 1. Total energy of chalcopyrite in ferromagnetic and antiferromagnetic states

	Energy/eV
Ferromagnetic	-11608.4359
Antiferromagnetic	-11609.9317

Table 2. Influence of U value on the cell parameters of antimagnetic chalcopyrite

U value/eV	Lattice parameters/ \AA
0	$a=b=5.1117, c=10.1564$
1.5	$a=b=5.2776, c=10.3803$
2.0	$a=b=5.2927, c=10.3875$
2.5	$a=b=5.3058, c=10.4058$
Experimental	$a=b=5.290, c=10.4217$

Notes: The experimental value is adopted by Knight et al. (2011)

Momosaki (1953) thought that covalent bonds have hydrophobic properties while electrostatic bonds have hydrophilic properties. The crystal structures of pyrite and chalcopyrite are compared in terms of Mulliken bond populations. The Mulliken bond populations (bond order) and lengths in pyrite and chalcopyrite are shown in Table 3. According to the Mulliken bond population, the covalent and ionic strength of the bond can be estimated. A higher Mulliken population value indicates a greater covalent bond (Segall et al., 1996). By comparing the bond populations in the chalcopyrite with those in the pyrite, it is found that the populations of Fe-S and Cu-S bonds in chalcopyrite are larger than those of S-S and Fe-S bonds in pyrite, whereas the Fe-S bond lengths are almost the same in these two minerals. This suggests that the covalency of chalcopyrite crystals is greater than that of pyrite crystals. The electron density map (Fig. 3) also clearly shows that the electron density distribution between Fe and S is more notable in chalcopyrite than in pyrite. In addition,

Table 3. Bond lengths and Mulliken populations in pyrite and chalcopyrite

	Bond	Length/ \AA	Mulliken population
Pyrite	Fe-S	2.247	0.33
	S-S	2.151	0.27
Chalcopyrite	Fe-S	2.250	0.50
	Cu-S	2.306	0.35

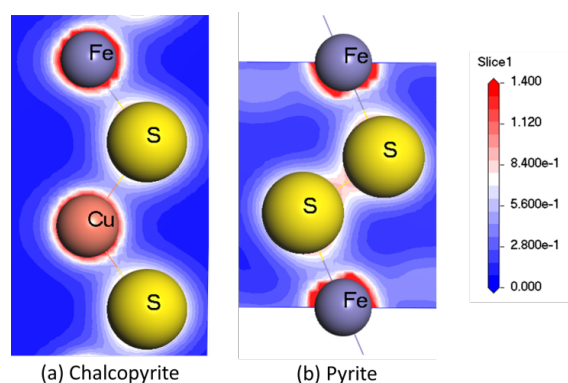


Fig. 3. Electron density maps of Cu-S and Fe-S bonds in chalcopyrite and S-S and Fe-S bonds in pyrite. The colour of the slice indicates the density

ion, in chalcopyrite, Fe-S bonds show greater covalent character than Cu-S bonds. Hence, the hydrophobicity of chalcopyrite will be greater than that of pyrite, which is conducive to the flotation of chalcopyrite.

3.2 Influence of Hubbard U correction on electronic structures

Flotation electrochemistry of sulphide minerals has been established based on the semiconducting properties of the minerals. Early studies have noted the influence of semiconductor types on the flotation of minerals. Eadington (1966) found that p-type galena oxidizes faster than n-type galena. Richardson et al. (1985) found that xanthate can react quickly on the surface of p-type galena, while the surface of n-type galena can adsorb xanthate only after it is oxidized. Both pyrite and chalcopyrite are typical semiconducting sulphide minerals, but they have different magnetic properties. Pyrite has a band gap of 1.01 eV at a U value of 1.5 eV, close to the experimental value of 0.95 eV (Schlegel and Wachter, 1976). Moreover, it is a p-type semiconductor and in the low-spin state due to the Fe 3d $t_{2g}^6e_g^0$ configuration. The calculations on pyrite are very extensive, and the results are of good consistency.

For chalcopyrite, there are many inconsistent results among its semiconducting properties. Oliveira et al. (2010) indicated a small indirect band gap of 0.1 eV by DFT-GGA calculations. Zhou et al. (2015) gave a band gap of 0.55 eV by using GGA+U with a U value of 3 eV for the 3d state of Fe, whereas Martínez-Casado et al. (2016) predicted a value of 1.82 eV by the DFT-B3LYP method. In addition, theoretical calculations often give conductive properties (Edelbro et al., 2003; Klekovkina et al., 2014). This is inconsistent with the experimental results that chalcopyrite has semiconducting properties (Goodman and Douglas, 1954, Austin et al., 1956). This may be because the calculations are based on ferromagnetic but not antiferromagnetic chalcopyrite. However, our GGA calculation on ferromagnetic or antiferromagnetic chalcopyrite also gives conductive properties. It is suggested that chalcopyrite exhibits semiconducting properties only when Hubbard U correction is used. This is consistent with the fact that chalcopyrite has been suggested to be an antiferromagnetic semiconductor material (Conejeros et al., 2015; Donnay et al., 1958; Woolley et al., 1996; Rais et al., 2000; Engin et al., 2011; Knight et al., 2011; Pearce et al., 2006).

Table 4 shows the effects of the U value on the band gap of antimagnetic chalcopyrite. The band gap increases gradually with increasing U values. When no U correction is used, the band gap of chalcopyrite is 0 eV, suggesting a metallic property of chalcopyrite. The band gap at a U value of 2.0 eV is 0.53 eV, which is very consistent with the experimental results of ~0.5 eV (Goodman and Douglas, 1954; Austin et al., 1956). Accordingly, a U value of 2.0 eV is determined to be suitable for chalcopyrite.

Table 4. Influence of the U value on the band gap of antimagnetic chalcopyrite

U value/eV	Band gap
0	0
1.5	0.36
2.0	0.53
2.5	0.74
Experimental	~0.5

Notes: The experimental value is adopted by Goodman and Douglas (1954) and Austin et al. (1956)

Fig. 4 shows the electronic band structures. It is indicated that both chalcopyrite and pyrite are indirect p-type semiconductors. For chalcopyrite, the valence band maximum and conduction band minimum are at the F-point and G-point, respectively. For pyrite, they are at the G-point and Z-point, respectively.

The spin-polarized calculations are performed for atoms, and the density of states (DOS) results of d spin up and spin down are depicted in Fig. 5. In pyrite, there is a high symmetry between the 3d up state and the 3d down state of the Fe atom, indicating the low spin state of the Fe atom. However, the Fe 3d up state and 3d down state in chalcopyrite are highly asymmetric, resulting in a spin magnetic

moment of Fe of 3.50 μB . This is close to the experimental and theoretical results. The experimental moment measured by Donnay et al. (1958) was 3.85 μB . Woolley et al. (1996) suggested 3.42 μB , and Engin et al. (2011) suggested 3.67 μB . The theoretically calculated values range from 3.80 to 3.93 (Conejeros et al., 2015; Hamajima et al., 1981; Fukushima et al., 2014). The Fe spin-up state contributes to the valence band, whereas the spin-down state mainly contributes to the conduction band. Some researchers have studied the effect of oxygen on mineral flotation (Chen et al., 2015; Sun et al., 2004). Because of the paramagnetic property of oxygen, the spin-polarized Fe atoms in the chalcopyrite are more likely to react with oxygen and be oxidized.

For the Cu atom in chalcopyrite, the symmetry between the 3d up state and the 3d down state is higher than that of the Fe atom. The net spin magnetic moment is 0.01 μB , and both the spin-up and spin-down states contribute to the valence band. Some researchers also gave small values for the Cu moment, which is very consistent with our result. Donnay et al. (1958) suggested that it is 0-0.2 μB according to the neutron diffraction results. Woolley et al. (1996) suggested approximately 0.05 μB for Cu at low temperature (50 K). Rais et al. (2000) proposed that Cu moments remain in a paramagnetic disordered state down to 190 K but are magnetic at lower temperatures.

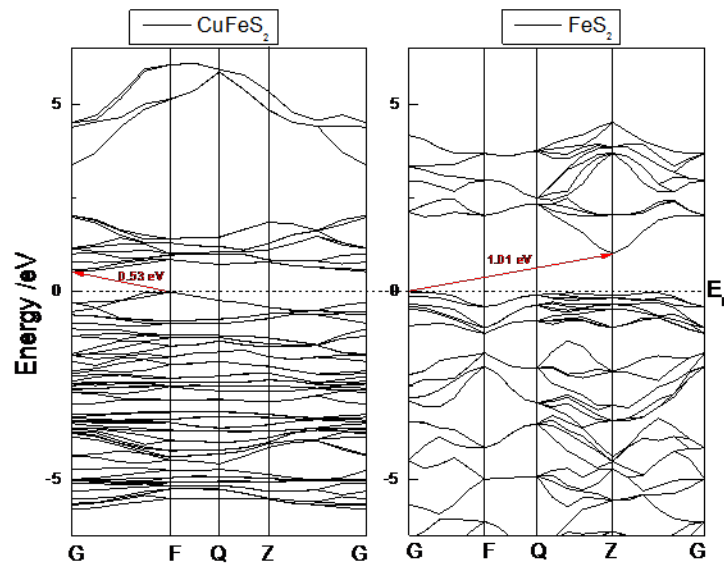


Fig. 4. Electronic band structures of chalcopyrite (a) and pyrite (b)

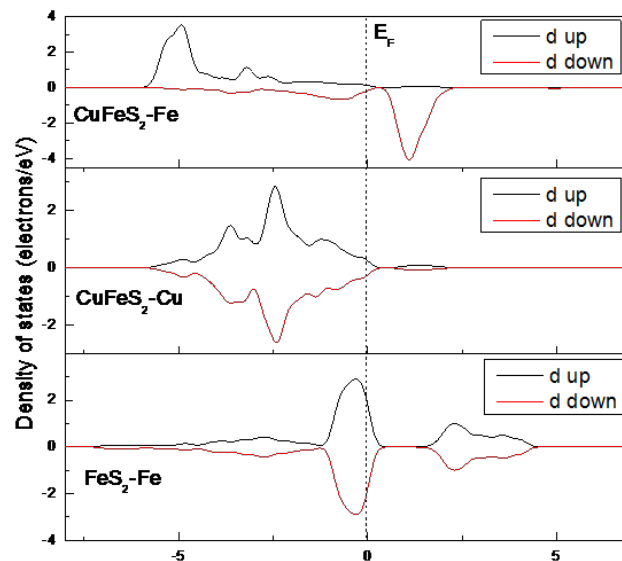


Fig. 5. Density of states of spin up and spin down depicted for Fe and Cu atoms. The Fermi level is set at the energy zero point

In addition to the spin DOS, the total and partial DOS of pyrite and chalcopyrite are also calculated, as shown in Fig. 6. The DOS of the S atom in pyrite is analogous to that in chalcopyrite. It is shown that the S s state contributes to the deep valence band and that the S p state contributes to the valence band near the Fermi level and the conduction band.

The DOS of the Fe atom in pyrite is very different from that in chalcopyrite. In pyrite, the Fe 3d state is separated on both sides of the Fermi level, whereas in chalcopyrite, it continuously passes through the Fermi level. In addition, the pyrite Fe 3d state peak next to the Fermi level in the valence band is very sharp, whereas in chalcopyrite, it is nonlocal. These results indicate that the pyrite Fe 3d state has stronger local properties than the chalcopyrite 3d state. In mineral flotation, when electrochemical reaction and adsorption occur, the atoms near the Fermi level have high reactivity and easily participate in the reaction. This indicates that Fe atoms in pyrite are more likely to exchange electrons with flotation agents than those in chalcopyrite.

Unlike the Fe 3d state, the Cu 3d state in chalcopyrite is only distributed in the valence band and is close to the Fermi level. Cu 4s and 4p states have the same energy level as Fe 4s and 4p states in the conduction band.

It is clear that, in chalcopyrite, the hybridization between Fe 3d and S 3p states is greater than that between Cu 3d and S 3p states, leading to the stronger covalent nature between Fe-S atoms than between Cu-S atoms. In addition, the hybridization between Fe 3d and S 3p states is also greater in chalcopyrite than in pyrite, resulting in the larger bond order and hence the greater covalency for Fe-S bonds in chalcopyrite than in pyrite. This is consistent with our previous analysis of the Mulliken populations.

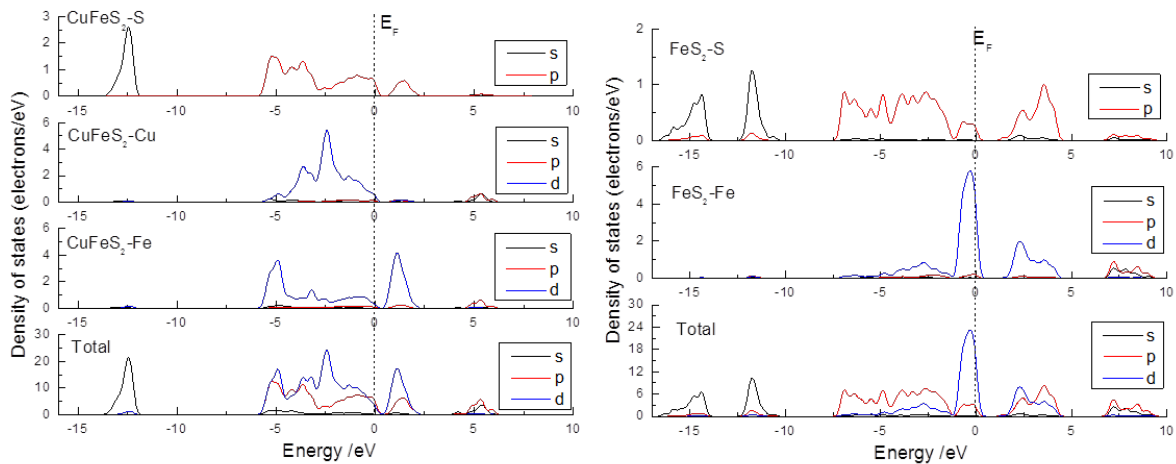


Fig. 6. Total and partial DOS of pyrite and chalcopyrite. The Fermi level is set at the energy zero point

For the ionic states of chalcopyrite, $\text{Cu}^+\text{Fe}^{3+}\text{S}_2^{2-}$, $\text{Cu}^{2+}\text{Fe}^{2+}\text{S}_2^{2-}$, and even the resonant configuration $\text{Cu}^+\text{Fe}^{3+}(\text{S}^{2-})-\text{Cu}^{3+}\text{Fe}(\text{S}^{2-})_2$ have been proposed based on X-ray spectroscopy (Ballal and Mande, 1978; Todd et al., 2003; Mikhlin et al., 2005) and the Mössbauer absorption spectrum (Aramu et al., 1967). The erroneous interpretation of $\text{Cu}^{2+}\text{Fe}^{2+}\text{S}_2^{2-}$ may be ascribed to the simplistic measurement method (Pearce et al., 2006). In the present work, the oxidation states of metal ions in chalcopyrite and pyrite were discussed and compared based on the coordination field theory according to the theoretical calculation results.

Cu and Fe atoms belong to the first transition metal elements. It is known that Fe and Cu atoms in CuFeS_2 are 4-coordinated, forming a tetrahedral configuration, and that Fe in FeS_2 is 6-coordinated, forming an octahedral configuration. Fig. 7 shows these two configurations.

The outer electronic arrangement for the Cu atom is $3d^{10}4s^14p^0$. According to the valence bond theory, when a metal ion is coordinated by ligands, sp^3 hybridization will make a tetrahedral configuration, so the Cu 3d orbital will not participate in sp^3 hybridization, retaining the $3d^{10}$ configuration to maintain a stable tetrahedral structure. Hence, in the CuS_4 tetrahedral field, the Cu atom will lose one electron to form the $3d^{10}4s^04p^0$ configuration, producing sp^3 hybrid orbitals to form

a tetrahedral configuration with four S atoms. Consequently, in CuFeS_2 , the valence state of Cu should be +1 but not +2. The low magnetic moment calculated for Cu ($0.01 \mu\text{B}$ of the spin magnetic moment) supports this result.

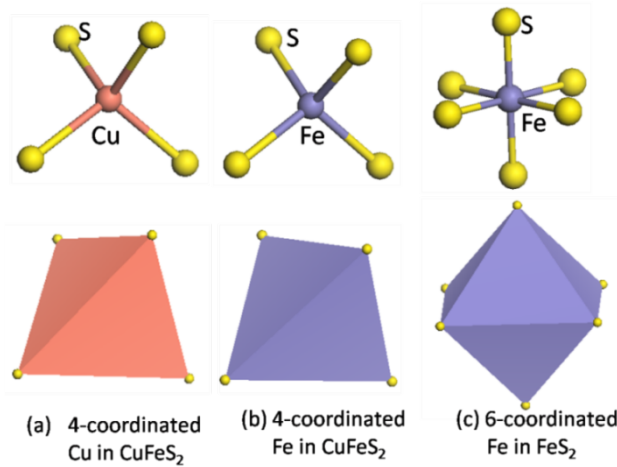


Fig. 7. Fe configurations in CuFeS_2 and FeS_2

The outer electronic arrangement for the Fe atom is $3d^64s^2$. For Fe in CuFeS_2 , our DOS calculation suggests that it is in a high-spin state with a moment of $3.50 \mu\text{B}$. This is in agreement with the coordination field theory that, in the regular tetrahedral field, Fe 3d electrons would be in a high-spin arrangement (weak field) because the electron pairing energy (P) is larger than their splitting energy (Δ). It is because $P > \Delta$ that the electrons in the Fe 3d orbital are easily lost, leading to the Fe ion in CuFeS_2 being in the $3d^5$ configuration (as shown in Fig. 8, the left pattern). However, for the Fe in FeS_2 , our DOS calculations are consistent with the crystal field theory (CFT) that Fe ions are in the low-spin state, where $P < \Delta$, and Fe ions have a $3d^6$ configuration with all of the electrons in pairs (the right pattern in Fig. 8).

Based on the above analysis, it is clear that the Fe in CuFeS_2 will be in the $3d^54s^0$ configuration, producing a +3 valence, compared to the $3d^64s^0$ configuration in FeS_2 with a +2 valence of Fe. Hence, the formal oxidation state for chalcopyrite should be $\text{Cu}^{+1}\text{Fe}^{+3}\text{S}_2^{2-}$, but not $\text{Cu}^{+2}\text{Fe}^{+2}\text{S}_2^{2-}$. This composition is consistent with the presence of high-spin Fe confirmed by Fe $L_{2,3}$ -edge X-ray absorption spectroscopy (XAS) along with Mössbauer data of chalcopyrite (Aramu et al., 1967) and is also consistent with our DOS calculation result that the Fe atom has a high spin magnetic moment of $3.50 \mu\text{B}$.

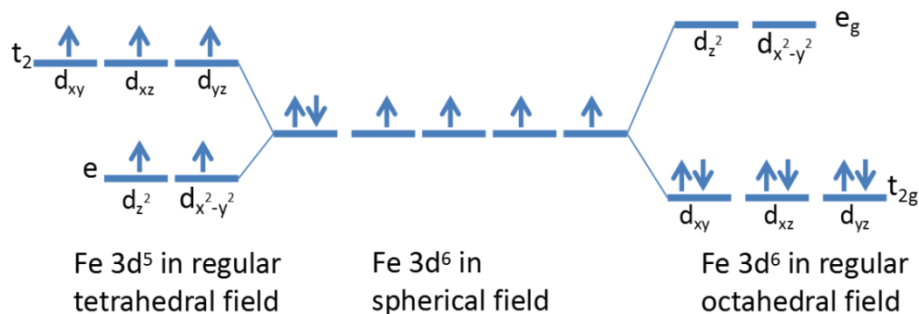


Fig. 8. Fe 3d electron configurations in different fields

It is also noted that the calculated magnetic moment of $3.50 \mu\text{B}$ for Fe^{3+} with the d^5 configuration is reduced from the ideal value of $5 \mu\text{B}$. It was proposed that strong Fe-S covalency caused a lower spin magnetic moment than the ideal value (Donnay et al., 1958, Fukushima et al., 2014). Our Mulliken bond population calculation verifies this result. The Fe-S bond order in chalcopyrite is 0.47, much larger than the 0.33 order in pyrite, suggesting stronger Fe-S covalency in chalcopyrite. The DOS

patterns (Fig. 6) clearly show that the hybridization between Fe 3d and S 3p states is greater in chalcopyrite than in pyrite. Through the above results, we held that chalcopyrite has stronger hydrophobicity than pyrite.

Furthermore, we studied the atomic activity in pyrite and chalcopyrite based on frontier molecular orbital (FMO) theory. FMO theory suggests that the reactivity of a molecule is determined by the highest occupied molecular orbital (HOMO) and the lowest unoccupied molecular orbital (LUMO). We calculated the Fermi level (E_F), energies of HOMO and LUMO, and orbital coefficients of atoms (Table 5). In electrochemical studies, the Fermi level (E_F) is used as the average chemical potential of electrons (Chen, 2015). The lower the Fermi level is, the higher the stability of electrons will be. As shown in Table 5, the Fermi level of pyrite (-5.768 eV) is close to that of chalcopyrite (-5.471 eV). This suggests that the electrochemical activity of pyrite is close to that of chalcopyrite. Allison et al. (1972) suggested that the resting potentials of pyrite (+0.22 V) and chalcopyrite (+0.14 V) were close in potassium ethyl xanthate at a pH of 7, and dixanthogen was the product for these two minerals.

In Table 5, only the orbitals with the largest coefficients are shown. The larger the orbital coefficient of an atom is, the greater the contribution of the atom to the frontier orbital will be. It is obvious that the contribution of Fe atoms to the LUMO of pyrite is larger than that to the HOMO, and S atoms contribute to both the HOMO and LUMO. For chalcopyrite, Fe 3d has the largest contribution to both the HOMO and LUMO orbitals, followed by S 3p and then Cu 3d.

Table 5. Fermi levels and orbital coefficients of pyrite and chalcopyrite

Mineral	Fermi level (eV)	Frontier orbital	Orbital coefficient
Pyrite	-5.768	HOMO	0.007 Fe 4p, 0.240 S 3p
		LUMO	0.419 Fe 3d, 0.136 S 3p, 0.291 S 3s
Chalcopyrite	-5.471	HOMO	0.455 Fe 3d, 0.098 Cu 3d, 0.157 S 3p
		LUMO	0.297 Fe 3d, 0.125 Cu 3d, 0.282 S3p, 0.037 S 3s

4. Conclusions

It is meaningful to study the different properties of chalcopyrite (Cu) and pyrite (S) to recover copper. Based on density functional theory (DFT) calculation, this study focused on the differences in crystal and electronic structures between these two minerals, which have not previously been thoroughly compared. The study results are helpful to confirm the crystal chemistry differences between chalcopyrite and pyrite and meaningful to study their flotation separation. Based on the research results obtained in this paper, the following can be summarized:

1. The Mulliken bond populations and lengths in pyrite and chalcopyrite indicate that the covalency of chalcopyrite crystals is greater than that of pyrite crystals, so the hydrophobicity of chalcopyrite is greater than that of pyrite.

2. The analysis of band structure and density functional theory (DFT) revealed that both chalcopyrite and pyrite belong to p-type semiconductors, and the hybridization between Fe 3d and S 3p states in chalcopyrite is stronger than that in pyrite. Hence, it is also suggested that the hydrophobicity of chalcopyrite is greater than that of pyrite.

3. In addition, antiferromagnetic calculations must be performed on chalcopyrite. When the U value is 2.0 eV, antiferromagnetic chalcopyrite is calculated to be a semiconductor with a band gap of 0.53 eV, which is very close to the experimental result (approximately 0.5 eV). The net spin magnetic moment calculated for Cu is 0.01 μ_B . The magnetic property of chalcopyrite is contributed by the Fe atom with 3.50 μ_B .

4. Based on the calculated results, the formal oxidation state of Cu and Fe in chalcopyrite is discussed. It is suggested that the oxidation states of Fe and Cu ions in chalcopyrite are $Fe^{3+}Cu^{1+}S_2$. This is very different from pyrite, which has formal oxidation states of $Fe^{2+}S_2$.

The present work focuses on the comparison of crystal structures and electronic structures of chalcopyrite and pyrite. Further studies will be carried out concerning the surface oxidation and the adsorption of flotation reagents on the surface. The results of the present work will help to explain the

results of oxidation and adsorption of the surfaces.

Acknowledgements

This research is financially supported by the National Natural Science Foundation of China (NSFC) (Nos. 51764002, 51974094 and 51874106) and the Guangxi Natural Science Foundation (2017GXNSFAA198216 and 2018GXNSFAA281355).

References

- ALLISON, S. A., GOOLD, L. A., NICOL, M. J., GRANVILLE, A., 1972. *A determination of the products of reaction between various sulfide minerals and aqueous xanthate solution, and a correlation of the products with electrode rest potentials*, Metallurgical and Materials Transaction B. 3(10), 2613-2618.
- ANISIMOV, V. I., 1995. *First-principles calculations of electronic structure and spectra of strongly correlated systems: LDA +U method*, Springer Series in Solid-State Sciences. 119, 106-116.
- ANISIMOV, V. I., ZAAANEN, J., ANDERSEN, O. K., 1991. *Band theory and Mott insulators: Hubbard U instead of Stoner I*, Physical Review B, Condensed Matter. 44(3), 943-954.
- ARAMU, F., BRESSANI, T., MANCA, P., 1967. *On the mössbauer effect of chalcopyrite*, II Nuovo Cimento B. 51, 370-375.
- AUSTIN, I. G., GOODMAN, C. H. L., PENGELLY, A. E., 1956. *New Semiconductors with the Chalcopyrite Structure*, Journal of the Electrochemical Society. 103(11), 609-610.
- BALLAL, M. M., MANDE, C., 1978. *X-ray spectroscopic study of some chalcopyrites*, Journal of Physics C Solid State Physics. 11(11), 837-848.
- CHEN, J., 2015. *The solide physics of sulphide minerals flotation*, Central South University Press, 24-28.
- CHEN, J.H., KE, B.L., LAN, L.H., LI, Y.Q., 2015. *DFT and experimental studies of oxygen adsorption on galena surface bearing Ag, Mn, Bi and Cu impurities*. Minerals Engineering. 71, 170-179.
- CLARK, S. J., SEGALLII, M. D., PICKARDII, C. J., HASNIPIII, P. J., PROBERTIV, M. I. J., 2005. *First principles methods using Castep*, Zeitschrift Für Kristallographie. 220(5-6), 567-570.
- CONEJEROS, S., ALEMANY, P., LLUNELL, M., MOREIRA, P. R., SANCHEZ, V., LLANOS, J., 2015. *Electronic structure and magnetic properties of CuFeS₂*, Inorganic Chemistry. 54, 4840-4849.
- DENG, Z.B., TONG, X., LOPEZ VALDIVIESO, A., WANG, X., XIE, X., 2015. *Collectorless flotation of marmatite with pine oil*. Rare Metals.
- DONNAY, G., CORLISS, L. M., DONNAY, J. D. H., ELLIOTT, N., HASTINGS, J. M., 1958. *Symmetry of magnetic structures: magnetic structure of chalcopyrite*, Physical Review. 112(6), 1917-1923.
- EADINGTON, P., 1966. *The oxidation of lead sulphide in aqueous suspension*. University of London.
- EDELBRO, R., SANDSTRÖM, A., PAUL, J., 2003. *Full potential calculations on the electron bandstructures of Sphalerite, Pyrite and Chalcopyrite*, Applied Surface Science. 206(1-4), 300-313.
- ENGIN, T. E., POWELL, A. V., HULL, S., 2011. *A high temperature diffraction-resistance study of chalcopyrite, CuFeS₂*, Journal of Solid State Chemistry. 184(8), 2272-2277.
- ENNAOUI, A., FIECHTER, C., PETTENKOFER, N., Alonso-Vante, N., Büker, K., Bronold, M., Höpfner, CH., Tributsch, H., 1993. *Iron disulfide for solar energy conversion*, Solar Energy Materials & Solar Cells. 29(4), 289-370.
- FUKUSHIMA, T., KATAYAMA-YOSHIDA, H., UEDE, H., TAKAWASHI, Y., NAKANISHI, A., SATO, K. J., 2014. *Computational materials design of negative effective U system in hole-doped chalcopyrite CuFeS₂*, Journal of Physics: Condensed Matter. 26, 355502.
- GOODMAN, C. H. L. and DOUGLAS, R. W., 1954. *New semiconducting compounds of diamond type structure*, Physica. 20(s7-12), 1107-1109.
- HAMAJIMA, T., KAMBARA, T., GONDAIRA, K. I., OGUCHI, T., 1981. *Self-consistent electronic structures of magnetic semiconductors by a discrete variational X calculation. III. Chalcopyrite CuFeS₂*, Physical Review B. 24(6), 3349-3353.
- HIROI, H., IWATA, Y., HORIGUCHI, K., SUGIMOTO, H., 2015. *960-mv open-circuit voltage chalcopyrite solar cell*, IEEE Journal of Photovoltaics. 6(1), 309-312.
- JAFFE, J. E., ZUNGER, A., 1983. *Electronic structure of the ternary chalcopyrite semiconductors CuAlS₂, CuGaS₂, CuInS₂, CuAlSe₂, CuGaSe₂, and CuInSe₂*, Physical Review B. 28(10), 5822-5847.
- KLEKOVKINA, V. V., GAINOV, R. R., VAGIZOV, F. G., DOOGLAV, A. V., GOLOVANEVSKIY, V. A., PEN'KOV, I. N., 2014. *Oxidation and magnetic states of chalcopyrite CuFeS₂: A first principles calculation*, Optics and

- Spectroscopy. 116(6), 885-888,
- KNIGHT, K. S., MARSHALL, W. G., ZOCHOWSKI, S. W., KEVIN, S., 2011. *The low-temperature and high-pressure thermoelastic and structural properties of chalcopyrite, CuFeS₂*, The Canadian Mineralogist. 49, 1012-1034.
- KRADINOVA, L. V., POLUBOTKO, A. M., POPOV, V. V., PROCHUKHAN, V. D., SKORIUKIN, V. E., 1999. *Novel zero-gap compounds, magnetics: CuFeS₂ and CuFeTe₂*, Semiconductor Science & Technology. 8(8), 1616-1619.
- LAZEWSKI, J., NEUMANN, H., PARLINSKI, K., 2004. *Ab initio characterization of magnetic CuFeS₂*, Physical Review B. 70(19), 3352-3359.
- LI, Y., CHEN, J., CHEN, Y., ZHAO, C., LEE, M. H., LIN, T. H., 2018. *DFT +U study on the electronic structures and optical properties of pyrite and marcasite*, Computational Materials Science. 150, 346-352.
- LI, Y., HE, Q., CHEN, J., ZHAO, C., 2015. *Electronic and chemical structures of pyrite and arsenopyrite*, Mineralogical Magazine. 79 (7) 1779-1789.
- LYUBUTIN, I. S., LIN, C. R., STARCHIKOV, S. S., 2013. *Synthesis, structural and magnetic properties of self-organized single-crystalline nanobricks of chalcopyrite CuFeS₂*, Acta Materialia. 61(11), 3956-3962.
- MARTÍNEZ-CASADO, R., CHEN, V. H. -Y., MALLIA, G., HARRISON, N. M., 2016. *A hybrid-exchange density functional study of the bonding and electronic structure in bulk CuFeS₂*, The Journal of Chemical Physics. 144(18), 184702.
- MARZARI, N., VANDERBILT, D., PAYNE, M. C., 1997. *Ensemble density-functional theory for Ab initio molecular dynamics of metals and Finite-temperature insulators*, Physical Review Letters. 79, 1337-1340.
- MIKHLIN, Y., TOMASHEVICH, Y., TAUSON, V., VYALIKH, D., MOLODTSOV, S., SZARGAN, R., 2005. *A comparative X-ray absorption near-edge structure study of bornite, Cu₅FeS₄, and chalcopyrite, CuFeS₂*, Journal of Electron Spectroscopy and Related Phenomena. 142, 83-88.
- MOMOSAKI J., 1953. *Some wetting Phenomena concerning Flotation*, Journal of the Mining and Metallurgical Institute of Japan. 69(781), 259-262.
- MU, Y., PENG, Y., LAUTEN, R. A., 2018. *The galvanic interaction between chalcopyrite and pyrite in the presence of lignosulfonate-based biopolymers and its effects on flotation performance*, Minerals Engineering. 122, 91-98.
- NAKAMURA, S., YAMAMOTO, A., 2001. *Electrodeposition of pyrite (FeS₂) thin films for photovoltaic cells*, Solar Energy Materials & Solar Cells. 65(1-4), 79-85.
- OLIVEIRA, C. D., DUARTE, H. A., 2010. *Disulphide and metal sulphide formation on the reconstructed (001) surface of chalcopyrite: A DFT study*, Applied Surface Science. 257, 1319-1324.
- PARK, S. J., CHO, Y., MOON, S. H., KIM, J. E., LEE, D. K., GWAK, J., KIM, J., KIM, D. K., MIN, B. K., 2014. *A comparative study of solution-processed low- and high-band-gap chalcopyrite thin-film solar cells*, Journal of Physics D: Applied Physics. 47(13) 135105.
- PAULING, L. and BROCKWAY, L. O., 1932. *The crystal structure of chalcopyrite CuFeS₂*, Zeitschrift Für Kristallographie - Crystalline Materials, 82, 1-6.
- PEARCE, C. I., PATTRICK, R. A. D., VAUGHAN, D. J., HENDERSON, C. M. B., LAAN, G. V. D., 2006. *Copper oxidation state in chalcopyrite: Mixed Cu d⁹ and d¹⁰ characteristics*, Geochimica Et Cosmochimica Acta. 70(18), 4635-4642.
- PRINCE, K. C., MATTEUCCI, M., KUEPPER, K., 2005. *Core-level spectroscopic study of FeO and FeS₂*, Physical Review B. 71, 085102.
- RAIS, A., GISMELSEED, A. M., AL-RAWAS, A. D., 2000. *Magnetic properties of natural chalcopyrite at low temperature*, Materials Letters. 46(6), 349-353.
- RICHARDSON, P.E., O'DELL, C.S., 1985. *Semiconducting characteristics of galena electrodes relationship to mineral flotation*. Journal of Electrochemical Society. 132(6), 1350-1356.
- SCHLEGEL, A. and WACHTER, P., 1976. *Optical properties, phonons and electronic structure of iron pyrite (FeS₂)*, Journal of Physics C: Solid State Physics. 9(17) 3363-3369.
- SIEBENTRITT, S., IGALSON, M., PERSSON, C., LANY, S., 2010. *The electronic structure of chalcopyrites – bands, point defects and grain boundaries*, Progress in Photovoltaics: Research Applications. 18(6), 390-410.
- SUN, W., HU, Y.H., QIU, G.Z., QIN, W.Q., 2004. *Oxygen adsorption on pyrite (100) surface by density functional theory*. Journal of Central South University of Technology. 11(004), 385-390.
- TERANISHI, T., 1961. *Magnetic and electric properties of chalcopyrite*, Journal of The Physical Society of Japan. 16(10), 1881-1887.
- TODD, E. C., SHERMAN, D. M., PURTON, J. A., 2003. *Surface oxidation of chalcopyrite (CuFeS₂) under ambient*

- atmospheric and aqueous (pH 2-10) conditions: Cu, Fe L- and O K- edge X-ray spectroscopy*, *Geochimica Et Cosmochimica Acta.* 67(12), 2137-2146.
- WOOLLEY, J. C., LAMARCHE, A. M., LAMARCHE, G., QUINTERO, M., SWAINSON, I. P., HOLDEN, T. M., 1996. *Low temperature magnetic behaviour of CuFeS₂ from neutron diffraction data*, *Journal of Magnetism and Magnetic Materials*, 162(2-3), 347-354.
- XI, P., WANG, D., LIU, W., SHI, C., 2019. *DFT study into the influence of carbon material on the hydrophobicity of a coal pyrite surface*, *Molecules.* 24(19), 3534.
- XIE, X., LU, D., 1998. *Energy band theory of solids*, Fudan University Press, 1-26.
- YU, L., LANY, S., KYKYNESHI, R., JIERATUM, V., RAVICHANDRAN, R., PELATT, B., ALTSCHUL, E., PLATT, H. A. S., WAGER, J. F., KESZLER, D. A., ZUNGER, A., 2011. *Iron chaocogenide photovoltaic absorbers*, *Advanced Energy Materials.* 1(5), 748-753.
- ZHOU, M., GAO, X., CHENG, Y., CHEN, X., CAI, L., 2015. *Structural, electronic, and elastic properties of CuFeS₂: First-principles study*, *Applied Physics A. Materials Science & Processing.* 118, 1145-1152.